Proceedings of the 2006 IASME/WSEAS International Conference on Continuum Mechanics, Chalkida, Greece, May 11-13, 2006 (pp191-196)

Thermodynamical modeling of ferroelectric polycrystalline material behavior

VOLKMAR MEHLING, CHARALAMPOS TSAKMAKIS, DIETMAR GROSS
Darmstadt University of Technology
Department of Civil Engineering
Hochschulstr. 1, 64289 Darmstadt
GERMANY

Abstract: A fully three-dimensional, thermodynamically consistent model for the behavior of polycrystalline ferroelectric ceramics, such as PZT or Barium Titanate is presented. In an internal variable framework, the internal state of the material is described by two microscopically motivated internal state variables. The first one is a second-order texture tensor, indicating the orientation of axes of the crystal unit cells. The second is vector-valued and describes the macroscopic polarization state. Similar to rate-independent plasticity theory for small deformations, strains and electric displacements are decomposed into reversible and irreversible parts. For the reversible part, a linear piezoelectric constitutive law is assumed. For the irreversible part, driving forces and evolution laws are established. Saturation and electro-mechanical coupling during irreversible processes are governed by energy barrier functions introduced in the electric enthalpy function. The model parameters are fitted to experimental hysteresis data. Illustrative examples demonstrate the models capabilities.

Key–Words: Piezoelectricity, Electromechanical Coupling, Ferroelectricity, Thermodynamical Modeling

1 Introduction

Piezoelectric materials exhibit electromechanically coupled behavior. Due to the direct piezoelectric effect, the polarization is altered by applied stresses, producing an electric signal. The so-called inverse piezoelectric effect causes the deformation of the material in an electric field. Both effects are used in various applications for sensoring and actuation. For small applied stresses and electric fields, the behavior of piezoelectrics is usually considered as reversible. Piezoelectric materials with the capability of repolarization under high electrical or mechanical fields are called ferroelectrics. The group of ferroelectrics, this paper is concerned with, exhibits the tetragonal phase of the perovskite crystal structure. The best known ferroelectrics are $BaTiO_3$ (Barium Titanate) and tetragonal PZT (Lead Zirconate Titanate). The latter is most frequently used for industrial application. The microscopic reason for repolarization is the switching from one state to another of unit cells or of domains with uniform orientation within the crystal . The domain switching process is dissipative such that the macroscopic behavior is hysteretic. For experimental results we refer to [10, 3, 13, 4]. The number of publications addressing the simulation of uni-axial behavior of ferroelectric materials is considerable. The development of reliable three-dimensional models is still subject to intensive research. For an overview of the literature the reader is referred to the review articles by Kamlah [6] and Landis [9]. The basic features of the model discussed in this paper have been presented in [11]. The current paper is intended to present the state of current research. The model partly relies upon previous works by Kamlah&Jiang [7] and Landis [8]. Analogous to the former, a set of internal state variables is chosen, which is motivated by microscopical considerations. Thermodynamical considerations are used to derive driving forces for the internal variables. Similarly to the proceeding in incremental plasticity theory, a loading function is used to divide reversible (piezoelectric) from irreversible (ferroelectric) processes. For the former, a linear piezoelectric relation is assumed, applying an invariant formulation cf. [12] including history dependent development of anisotropy for the mechanical, the electrical as well as for the piezoelectric coupling properties. For the latter, normality rules are used to determine the rates of change of internal state variables. Energy barrier functions

are used to model the saturation of irreversible strain and polarization, the saturation states being defined by the boundaries of the admissible range of the internal state variables.

2 Notation

When index notation is applied, it refers to a cartesian frame of reference and the indices are denoted by small, slanted letters. Use is made of the summation convention. Scalars are denoted by slanted letters (H, α,...), vectors are marked by arrows ($\vec{\mathrm{P}}, \vec{\mathrm{n}}$,...), while second, third and fourth order tensors are represented by bold face ($\mathbf{A}, \boldsymbol{\sigma}$,...), small double- stroke ($\mathbb{d}, \mathbb{e}$,...) and capital double-stroke letters ($\mathbb{C}, \mathbb{P}$,...), respectively. The rules $\vec{\mathrm{a}}\cdot\vec{\mathrm{b}} = a_i b_i$, $\mathrm{tr}\,(\mathbf{A}) = A_{kk}$, $(\mathbb{a}\cdot\vec{\mathrm{b}})_{ij} = a_{ijk} b_k$, $(\mathbb{a}:\mathbf{B})_k = a_{kij} B_{ij}$, $(\mathbf{A}\cdot\mathbf{B})_{ij} = A_{ik} B_{kj}$, $(\mathbf{A}^{\mathrm{T}})_{ij} = A_{ji}$, $\mathbf{A}:\mathbf{B} = \mathrm{tr}(\mathbf{A}\cdot\mathbf{B}^{\mathrm{T}})$, $(\mathbb{a}^{\mathrm{T}})_{ijk} = a_{kij}$ and $(\mathbb{C}:\mathbf{A})_{ij} = C_{ijkl} A_{kl}$ hold, while $|\vec{\mathrm{a}}| = \sqrt{\vec{\mathrm{a}}\cdot\vec{\mathrm{a}}}$ is the EUCLIDEAN norm of the vector $\vec{\mathrm{a}}$ and $\mathrm{dev}\,\mathbf{A}$ is the deviator of $\mathbf{A}$. We denote by $\vec{\mathrm{a}}\otimes\vec{\mathrm{b}}$ the tensorial product of two vectors $\vec{\mathrm{a}}$ and $\vec{\mathrm{b}}$. Thus, e.g. $\vec{\mathrm{a}}\otimes\mathbf{B}$ represents a third-order tensor. Let A be a function of B. For the partial derivative with respect to B, we write $\partial_B A$, while $\dot{(\cdot)}$ is the material time derivative of $(\cdot)$. The divergence and gradient operators are $\mathrm{div}\,(\cdot)$ and $\mathrm{grad}\,(\cdot)$.

3 Model Summary

3.1 Thermodynamical Considerations

We start from the balance equations for mass, linear and angular momentum, energy, entropy, electric charge and magnetic flux. Neglecting electric body forces and couples [6], as well as mechanical body forces, the balance equations of linear and angular momentum reduce to $\mathrm{div}\,\boldsymbol{\sigma} = 0$, where $\boldsymbol{\sigma}$ is the symmetric CAUCHY stress tensor. We restrict ourselves to quasi-electrostatic processes and assume perfectly insulating properties. Then, in the absence of external charges, the MAXWELL-relations reduce to $\mathrm{div}\,\vec{\mathrm{D}} = 0$, and there exists an electric potential function φ, such that $\vec{\mathrm{E}} = -\,\mathrm{grad}\,\varphi$. Here, $\vec{\mathrm{D}}$ and $\vec{\mathrm{E}}$ denote the electric displacement and the electric field strength, respectively. The above field equations are supplemented by the NEUMANN-boundary conditions $\boldsymbol{\sigma}\cdot\vec{\mathrm{n}} = \vec{\mathrm{t}}$ and $\vec{\mathrm{D}}\cdot\vec{\mathrm{n}} = q^{\mathrm{f}}$ on surfaces with prescribed tractions $\vec{\mathrm{t}}$ or prescribed free charge densities q^{f} and with surface normals $\vec{\mathrm{n}}$, and by the DIRICHLET-conditions for surfaces with prescribed displacements $\vec{\mathrm{u}}$ or electric potentials φ.

Assuming, that the entropy flux and source terms are linked to the heat flux and radiation by the absolute temperature, and demanding the entropy production to be positive for all processes, one arrives at the CLAUSIUS-DUHEM inequality

$$\varrho\dot{\psi} + \varrho\dot{\theta}s - \dot{\boldsymbol{\varepsilon}}\cdot\boldsymbol{\sigma} - \varrho p^{\mathrm{e}} + \frac{1}{\theta}\vec{\mathrm{q}}\cdot\,\mathrm{grad}\,\theta = -\varrho\pi_s \le 0, \quad (1)$$

where ψ is the HELMHOLTZ free energy, ϱ denotes the mass density, θ and s are the absolute temperature and the entropy, respectively. $\dot{\boldsymbol{\varepsilon}}$ and $\boldsymbol{\sigma}$ denote the strain rate and CAUCHY stress, p^{e} is the electrical power, $\vec{\mathrm{q}}$ is the heat flux vector and π_s is the entropy production. Now, the following assumptions are made:

- We consider isothermal processes with small deformations and uniform distribution of temperature.
- The material properties are assumed as time-independent.
- The electric enthalpy H, which is introduced by a LEGENDRE transform

$$\varrho\dot{H} = \varrho\dot{\psi} - \dot{\vec{\mathrm{E}}}\cdot\vec{\mathrm{D}} - \vec{\mathrm{E}}\cdot\dot{\vec{\mathrm{D}}}, \quad (2)$$

  is a function of the electric Field $\vec{\mathrm{E}}$, the strain $\boldsymbol{\varepsilon}$ and a set of internal state variables $\mathbf{q}$. Furthermore it is assumed to be additively decomposable into two parts, H^{r} and H^{i}, where H^{i} only depends on $\mathbf{q}$

$$H = \bar{H}(\boldsymbol{\varepsilon}, \vec{\mathrm{E}}, \mathbf{q}) = H^{\mathrm{r}} + H^{\mathrm{i}} \quad (3)$$

$$H^{\mathrm{r}} = \bar{H}^{\mathrm{r}}(\boldsymbol{\varepsilon}, \vec{\mathrm{E}}, \mathbf{q}) \;,\quad H^{\mathrm{i}} = \bar{H}^{\mathrm{i}}(\mathbf{q}) \;. \quad (4)$$

With this, equation (1) can be rewritten in terms of H as

$$\left(\boldsymbol{\sigma} - \varrho\partial_{\boldsymbol{\varepsilon}}\bar{H}\right) : \dot{\boldsymbol{\varepsilon}} - \left(\vec{\mathrm{D}} + \varrho\partial_{\vec{\mathrm{E}}}\bar{H}\right)\cdot\dot{\vec{\mathrm{E}}} - \sum_j \varrho\partial_{q_j}\bar{H}\dot{q}_j \;\ge\; 0 \;. \quad (5)$$

Applying standard arguments of thermodynamics, it follows, that

$$\boldsymbol{\sigma} = \varrho\partial_{\boldsymbol{\varepsilon}}\bar{H}^{\mathrm{r}} \quad \text{and} \quad \vec{\mathrm{D}} = -\varrho\partial_{\vec{\mathrm{E}}}\bar{H}^{\mathrm{r}} \;, \quad (6)$$

together with the dissipation inequality

$$\dot{\mathcal{D}} := \sum_j (-\varrho\partial_{q_j}\bar{H})\dot{q}_j \ge 0 \quad (7)$$

are sufficient conditions for the validity of the second law of thermodynamics in the form of the CLAUSIUS–DUHEM inequality for every admissible process.

3.2 Internal State Variables

The following additive decompositions into reversible and irreversible parts of the strain tensor $\boldsymbol{\varepsilon}$ and the electric displacement $\vec{\mathrm{D}}$ are assumed to apply (cf. e.g. [2]):

$$\boldsymbol{\varepsilon} \;=\; \boldsymbol{\varepsilon}^{\mathrm{r}} + \boldsymbol{\varepsilon}^{\mathrm{i}} \quad , \quad \vec{\mathrm{D}} \;=\; \vec{\mathrm{D}}^{\mathrm{r}} + \vec{\mathrm{P}}^{\mathrm{i}} \; . \tag{8}$$

Here it is assumed, that $\boldsymbol{\varepsilon}^{\mathrm{i}}$ and $\vec{\mathrm{P}}^{\mathrm{i}}$ are functions of $\mathbf{q}$ (cf. [7]):

$$\boldsymbol{\varepsilon}^{\mathrm{i}} = \hat{\boldsymbol{\varepsilon}}^{\mathrm{i}}(q_j), \qquad \vec{\mathrm{P}}^{\mathrm{i}} = \hat{\vec{\mathrm{P}}}^{\mathrm{i}}(q_j) \; . \tag{9}$$

For the polycrystalline ferroelectrics with tetragonal crystal structure considered here, the crystal unit cells can be characterized by the orientation of their longer crystal axis, in the following referred to as 'c-axis' and by the direction of the spontaneous polarization of that cell. Note, that a cell with a given c-axis may be polarized only parallel to this axis. In particular, with $\vec{c}$ denoting the direction of the c-axis, the polarization can be $\pm P_s \vec{c}$, where the material constant P_s is the magnitude of spontaneous polarization. We define the orientation distribution function (ODF)

$$f = \frac{3}{4\pi} \vec{c} \cdot \mathbf{A} \cdot \vec{c} \; , \tag{10}$$

where $\mathbf{A}$ is referred to as the *texture tensor* of the distribution and denotes a symmetric, positive semi-definite second-order tensor, with $\mathrm{tr}\,(\mathbf{A}) = 1$. Function f can be interpreted as a surface-density function on the unit sphere. Then, integration over all directions $\vec{c}$ yields $\iint f \; \mathrm{d}A = 1$.

The irreversible strain state of a unit cell is directly connected to the direction of its c-axis. In [11], volume averaging over all unit cells is used to derive the macroscopic irreversible strain

$$\boldsymbol{\varepsilon}^{\mathrm{i}} \;=\; \frac{3}{2} \varepsilon_0 \left(\mathbf{A} - \frac{1}{3} \mathbf{1} \right) \; . \tag{11}$$

The texture tensor $\mathbf{A}$ serves as an internal state variable, that describes the irreversible strain state. An irreversible strain state is considered as saturated, if one or two eigenvalues of $\mathbf{A}$ equal zero. For the representation of the macroscopic remanent polarization, a vector-valued state variable $\vec{\mathrm{p}}$ is chosen, such that

$$\vec{\mathrm{P}}^{\mathrm{i}} = P_0 \vec{\mathrm{p}} \; . \tag{12}$$

ε_0 and P_0 are the saturation values of uniaxial strain and polarization of the polycrystal. The extent to which the material can be polarized depends on the orientation of c-axes. It has been shown in [11], that the texture-dependent limit states (saturation states) of polarization in a given direction $\vec{\mathrm{n}}$, $|\vec{\mathrm{n}}| = 1$ can be expressed by the polarizability function

$$\vec{\mathrm{P}}^{\mathrm{i}}_{\mathrm{sat}} = P_0 \left(\mathbf{A} \cdot \vec{\mathrm{n}} + \frac{1}{2} \left(1 - \vec{\mathrm{n}} \cdot \mathbf{A} \cdot \vec{\mathrm{n}} \right) \vec{\mathrm{n}} \right) . \tag{13}$$

This function is comparable to the 'distance variable' applied in [8]. For simplicity, (13) is approximated by an ellipsoidal form

$$\vec{\mathrm{P}}^{\mathrm{i}\,\star}_{\mathrm{sat}} = \frac{1}{2} P_0 \left(\mathbf{1} + \mathbf{A} \right) \cdot \vec{\mathrm{n}} \; , \quad |\vec{\mathrm{n}}| = 1 \; . \tag{14}$$

The admissible range for $\vec{\mathrm{p}}$ can be written as

$$\left\{ \vec{\mathrm{p}} \;\middle|\; |2(\mathbf{1} + \mathbf{A})^{-1} \cdot \vec{\mathrm{p}}| \leq 1 \right\} \; , \tag{15}$$

and the distance of the relative polarization from the saturation surface can be described by the variable

$$\eta = 2|(\mathbf{1} + \mathbf{A})^{-1} \cdot \vec{\mathrm{p}}| \; . \tag{16}$$

It is zero for vanishing polarization and equal to one in case of polarization saturation.

3.3 Constitutive Law

When leaving the switching processes out of consideration, the behavior of ferroelectrics is purely piezoelectric. It is common, to assume the piezoelectric relation between the mechanical and electrical state variables to be linear (e.g. [5]). In our case the piezoelectric part of the electric enthalpy function is formulated by application of an invariant scheme. It can be written in the following quadratic form

$$\begin{aligned} \varrho H^{\mathrm{r}} \;&=\; \varrho \bar{H}^{\mathrm{r}}(\hat{\boldsymbol{\varepsilon}}^{\mathrm{r}}(\boldsymbol{\varepsilon}, \mathbf{A}), \vec{\mathrm{E}}, \vec{\mathrm{p}}) \qquad (17) \\ &= \frac{1}{2} \boldsymbol{\varepsilon}^{\mathrm{r}} \!:\! \mathbb{C}^{\mathrm{E}}(\vec{\mathrm{p}}) \!:\! \boldsymbol{\varepsilon}^{\mathrm{r}} - \boldsymbol{\varepsilon}^{\mathrm{r}} \!:\! \mathfrak{e}(\vec{\mathrm{p}}) \cdot \vec{\mathrm{E}} - \frac{1}{2} \vec{\mathrm{E}} \cdot \boldsymbol{\epsilon}^{\varepsilon}(\vec{\mathrm{p}}) \cdot \vec{\mathrm{E}} - \vec{\mathrm{P}}^{\mathrm{i}} \cdot \vec{\mathrm{E}} \; , \end{aligned}$$

with the tensors of elastic, piezoelectric and dielectric moduli $\mathbb{C}^{\mathrm{E}}$, $\mathfrak{e}$ and $\boldsymbol{\epsilon}^{\varepsilon}$, respectively, being functions of the polarization state of the polycrystal. In this sense, the piezoelectric relation is assumed to be transversely isotropic, with the axis of anisotropy aligned with the vector of irreversible macroscopic polarization. For vanishing macroscopic polarization (i.e. $|\vec{\mathrm{p}}| = \vec{0}$) all moduli become isotropic and piezoelectric coupling disappears. This seems reasonable for the thermally depolarized state of the polycrystal.

Similarly to [7] and [8] the part of the electric enthalpy function, which is concerned with irreversible processes is composed of quadratic functions, and singular terms, which tend to infinity as internal variables approach saturation states:

$$\begin{aligned} \varrho H^{\mathrm{i}} &= \varrho \hat{H}^{\mathrm{i}}(\mathbf{A}, \vec{\mathrm{p}}) \qquad (18) \\ &= \frac{1}{2} c_{\mathrm{A}} \mathrm{tr}\, \mathrm{dev}\, (\mathbf{A})^2 + \frac{1}{2} c_{\mathrm{p}} \vec{\mathrm{p}} \cdot \vec{\mathrm{p}} \\ &+ \frac{a_{\mathrm{A}}}{m_{\mathrm{A}}} \mathrm{tr}\, (\mathbf{A}^{-m_{\mathrm{A}}}) + \frac{a_{\mathrm{p}}}{m_{\mathrm{p}}} (1-\eta)^{-m_{\mathrm{p}}} \qquad (19) \end{aligned}$$

The third term on the right hand side of (18) represents an energy barrier function, which accounts for strain saturation. It grows to infinity as any eigenvalue of the texture tensor approaches zero. Analogously, the last term tends to infinity as the gap between the current amount of polarization and the polarizability vanishes. $c_{\mathrm{A}}, a_{\mathrm{A}}, c_{\mathrm{p}}, a_{\mathrm{p}}, m_{\mathrm{A}}$ and m_{p} are material parameters.

Using the above definitions, we can identify the terms in the brackets of equation (7) as driving forces $\mathbf{f}^{\mathrm{A}}$ and $\vec{\mathrm{f}}^{\mathrm{p}}$ for the internal variables $\mathbf{A}$ and $\vec{\mathrm{p}}$.

$$\begin{aligned} \mathbf{f}^{\mathrm{A}} &= -\varrho \partial_{\mathbf{A}} \hat{H}^{\mathrm{i}} \,, \\ \vec{\mathrm{f}}^{\mathrm{p}} &= -\varrho \partial_{\vec{\mathrm{p}}} \hat{H}^{\mathrm{r}} - \varrho \partial_{\vec{\mathrm{p}}} \hat{H}^{\mathrm{i}} . \end{aligned} \qquad (20)$$

Well motivated by the experimental observation, namely that irreversible processes only occur in case of loading beyond certain limits, a so-called switching function is introduced to distinguish reversible from irreversible processes. It is completely analogous to yield functions in plasticity theory. In particular, the following switching function is used in the examples below,

$$\begin{aligned} F = & \frac{\mathrm{dev}\,(\mathbf{f}^{\mathrm{A}})}{f_{\mathrm{c}}^{\mathrm{A}}} : \frac{\mathrm{dev}\,(\mathbf{f}^{\mathrm{A}})}{f_{\mathrm{c}}^{\mathrm{A}}} + \frac{\mathrm{dev}\,(\mathbf{f}^{\mathrm{A}})}{f_{\mathrm{c}}^{\mathrm{A}}} : (\vec{\mathrm{p}} \otimes \frac{\vec{\mathrm{f}}^{\mathrm{p}}}{f_{\mathrm{c}}^{\mathrm{p}}})_{\mathrm{sym}} \\ & + \frac{|\vec{\mathrm{f}}^{\mathrm{p}}|^2}{(f_{\mathrm{c}}^{\mathrm{p}})^2} - 1 \,, \end{aligned} \qquad (21)$$

where $f_{\mathrm{c}}^{\mathrm{A}} = \sqrt{1.5}\varepsilon_0 \sigma_{\mathrm{c}}$ and $f_{\mathrm{c}}^{\mathrm{p}} = P_0 E_{\mathrm{c}}$ represent critical driving forces in uniaxial experiments. In these equations, E_{c} and σ_{c} are the coercive electric field and the coercive stress, respectively. The postulation of maximum electro-mechanical dissipation during switching processes leads to the normality rules for the evolution of the internal state variables

$$\dot{\mathbf{A}} = \dot{\lambda} \partial_{\mathbf{f}^{\mathrm{A}}} F \,, \quad \dot{\vec{\mathrm{p}}} = \dot{\lambda} \partial_{\vec{\mathrm{f}}^{\mathrm{p}}} F \,. \qquad (22)$$

The factor $\dot{\lambda}$ is determined from the so-called consistency condition $\dot{F} = 0$.

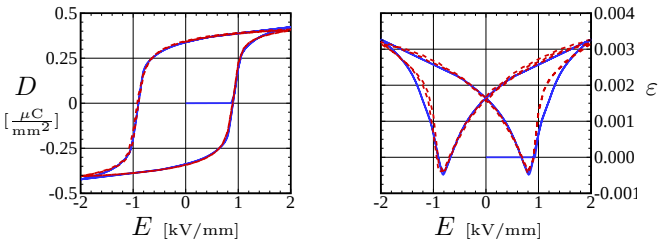

Figure 1: Experimentally observed (dashed lines) and simulated (solid lines) D-E (left) and ε-E (right) hysteresis loops.

4 Numerical Simulations

The model has been implemented in a finite element code to facilitate the simulation of complex non-homogeneous setups. The calculations have been carried out using the MatLab based open-source finite element code DAEdalon (www.daedalon.org), employing three displacement components and the electric potential as nodal degrees of freedom. Time-integration of the rate-equations is carried out by the backward-Euler scheme together with the predictor-corrector method known from computational plasticity.

The parameters of the model have been roughly fitted to experimental hysteresis data from uniaxial electric cycling [1]. The measured and simulated hysteresis loops are depicted in Fig.1. The agreement of both sets of graphs is very good, though some discrepancy remains in the strain hysteresis. It is clear, however, that additional effort and more data, e.g. from purely mechanical experiments, are required, to fit all parameters in a satisfying way.

In Fig.2, the model behavior for different types of uniaxial loading is shown. All of these are in good qualitative agreement with experimental observations reported e.g. in [3, 10, 13]. Figs.2a and b show the model response to electric cyclic loading with different superimposed constant mechanical stresses. Compared to the case without the mechanical loading, one can observe, that small compressive stresses (-15MPa) increase the ratio of maximum to minimum strain, while high stresses inhibit the evaluation of texture and thus lead to degenerated butterfly hysteresis loops. Accordingly, the electric hysteresis loop for high compressive stress is reduced to the part which is related to pure 180° switching (change of polarization without change of texture). During mechanical depolarization (Fig.2c and d), a previously polarized ferroelectric is sub-

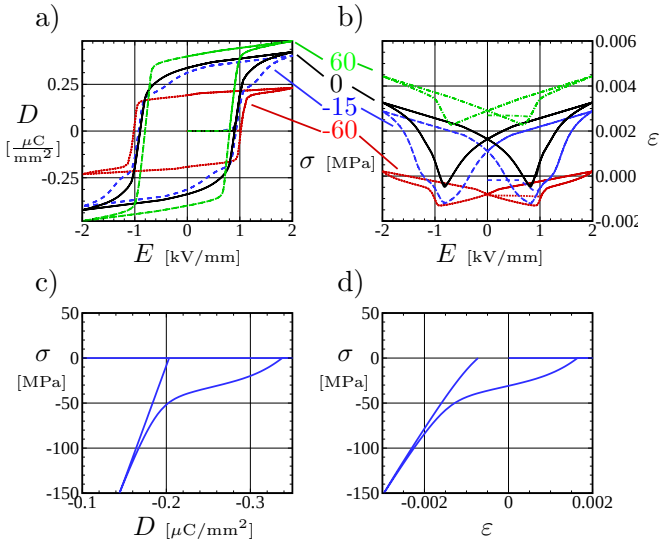

Figure 2: Model response a) $D-E$-hysteresis loops for different magnitudes of superimposed constant stress. b) butterfly hysteresis connected with a). c) total strain during depolarization by compressive stress. d) polarization during depolarization.

jected to compressive stress along the axis of original poling. Thereby, the material is partly depolarized, accompanied by a negative irreversible strain.

The graphs in Fig.3 resemble the multiaxial polarization rotation experiment reported in [4]. Here, a previously poled ferroelectric is subjected to an electric field, which differs from the original poling direction by different angles

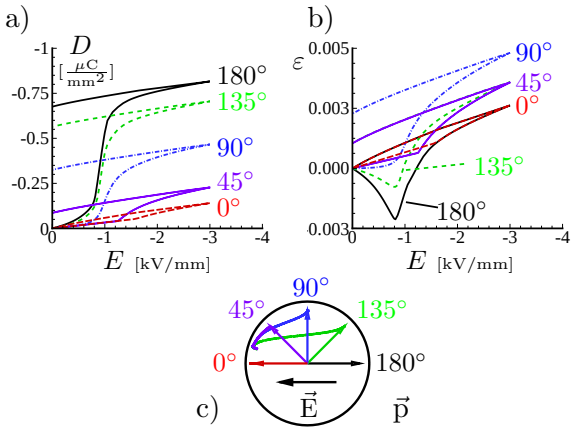

Figure 3: Polarization rotation: electric loading, with the original poling direction differing by α from the direction of the applied electric field. a) electric response, b) strain response, c) evolution of relative polarization.

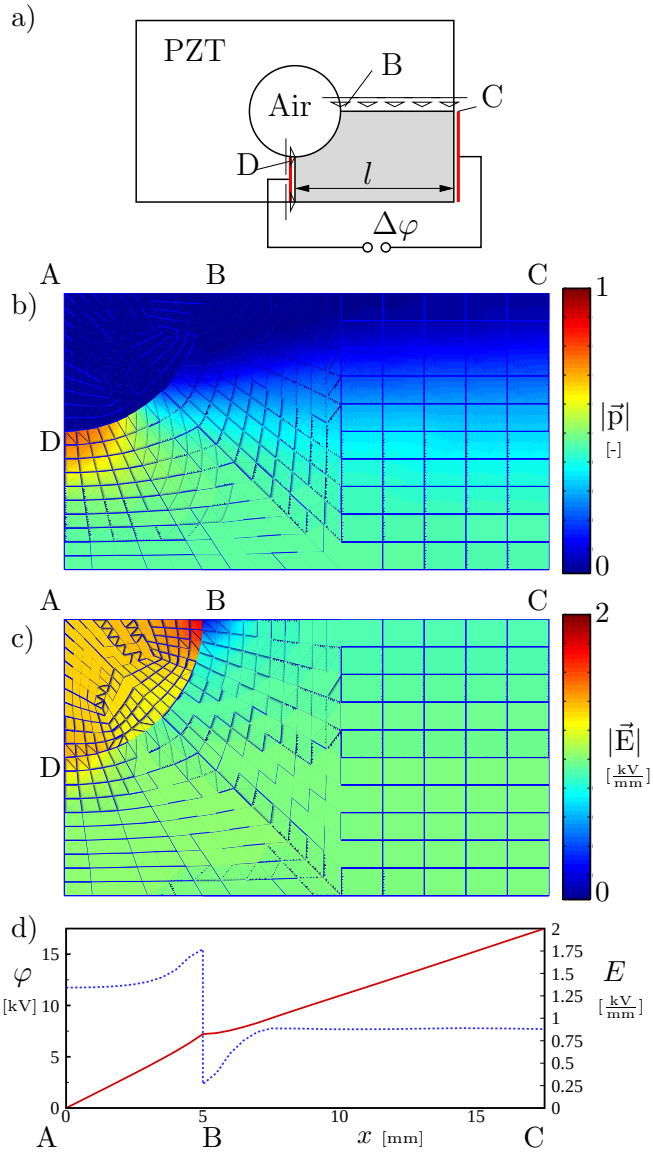

Figure 4: a) Schematics of the simulation of a quarter of a strip with a circular hole. The potential boundary conditions are applied to the left and right boundaries. b) Contour plot of the magnitude of relative irreversible polarization $|\vec{p}|$. Maximum value is 0.78 at point D. c) Contour plot of the magnitude of the electric field $|\vec{E}|$, Maximum value inside the hole is 1.77 kV/mm at point B, in the ferroelectric 1.38 kV/mm at point D. d) Electric potential φ (solid line) and electric field strength E (dotted line) along the line of symmetry A-B-C at an average electric field of 1kV/mm.

$\alpha = 0°, 45°, 90°, 135°$ and $180°$. The response strongly depends on α. The change in electric displacement D is increasing with increasing an-

gles, the change in strain is largest for $\alpha = 90°$. For $\alpha = 180°$, the results are exactly one half of the hysteresis loops in Fig.1. The small graph in Fig.3c depicts the evolution of relative polarization, starting from the different initial states, indicated by the arrows. The applied electric field is pointing to the left.

The aim of the last example (Fig.4) is to demonstrate the capability of the model to predict complex inhomogeneous loading states. An initially unpolarized ferroelectric strip (PZT) with a circular hole (35×20mm) has electrodes attached to its short ends. The hole is modelled as dielectric (air/vacuum). To reduce the calculation effort, only one quarter of the system is discetized (see Fig.4a). The potential difference $\Delta\varphi$ is increased linearly from zero to 17.5 kV (for the quarter system). Thus, the average electric field strength at the final state of loading is 1 kV/mm, which is slightly above the coercive field of 0.9 kV/mm. It becomes clear, that the electric field inside of the hole is much higher than the one in the ferroelectric. For comparison the same calculations have been carried out without discretization the hole, i.e. with a free surface on the interface. The results are almost identical to the ones presented in this paper. This indicates, that there is no need to account for the dielectric properties of the air in the hole. However, one should keep in mind, that high electric fields could lead do electric discharge in an experimental setup.

5 Conclusion

A constitutive model has been presented, which accounts for multi-axial switching and its capabilities to reproduce experimental results have been demonstrated. The more elaborated fitting of all constitutive parameters remains a difficult and laborious task and is beyond the scope of this work. The restriction to materials with tetragonal structure is convenient. However, the proceeding could be generalized for other or additional structures.

Acknowledgements: We thank N. Balke and J. Rödel of the Department of Material Sciences at the Darmstadt University of Technology for providing experimental data.

References:

[1] N. Balke, D.C. Lupascu, T. Granzow and J.Rödel. Unipolar fatigue and dc loading of lead zirconate titanate ceramics. Acta. Mater, submitted. 2006.

[2] E. Bassiouny, A.F. Ghaleb and G.A. Maugin. Thermomechanical formulation for coupled electromechanical hysteresis effects – I. Basic equations, II. Poling of ceramics. Int. J. of Eng. Sci., **26**,1279–1306, 1988.

[3] T. Fett, S. Müller, D. Munz and G. Thun. Nonsymmetry in the deformation behaviour of PZT. J. of Mater. Sci. Lett., **17**,261–265, 1998.

[4] J.E. Huber and N.A. Fleck. Multi-axial electric switching of a ferroelectric: theory versus experiment. J. Mech. Phys. Sol., **49**,785–811, 2001.

[5] B. Jaffe, W. R. Cook and H. Jaffe. *Piezoelectric Ceramics*, Academic Press, London, 1964.

[6] M. Kamlah. Ferroelectric and ferroelastic piezoceramics - modeling of electromechanical hysteresis phenomena. Cont. Mech. Thermodyn., **13**(4),219–268, 2001.

[7] M. Kamlah and Q. Jiang. A constitutive model for ferroelectric PZT ceramics under uniaxial loading. Smart Mater. Struct., **8**,441–459, 1999.

[8] C.M. Landis. Fully coupled, multi-axial, symmetric constitutive laws for polycrystalline ferroelectric ceramics. J. Mech. Phys. Sol., **50**,127–152, 2002.

[9] C.M. Landis. Non-linear constitutive modeling of ferroelectrics. Curr. Op. Sol. St. Mater. Sci., **8**,59–69, 2004.

[10] C.S. Lynch. The effect of uniaxial stress on the electro-mechanical response of 8/65/35 PLZT. Acta mater., **44**(10),4137–4148, 1996.

[11] V. Mehling and Ch. Tsakmakis and D. Gross, A simple fully coupled three-dimensional phenomenological model for ferroelectric ceramics, Coupled Problems, 2005, M. Papadrakis and E. Oñate and B. Schrefler, (Edts.), CIMNE, Barcelona,

[12] J. Schröder and D. Gross. Invariant formulation of the electromechanical enthalpy function of transversely isotropic piezoelectric materials. Arch. Appl. Mech., **73**,533–552, 2004.

[13] D. Zhou. *Experimental investigation of nonlinear constitutive behavior of PZT piezoceramics*. Dissertation, University of Karlsruhe(TH), FZ Karlsruhe, 2003.